Lasers in Manufacturing Conference 2017

Quantitative identification of laser cutting quality relying on visual information

M. Pacher[a, *], L. Monguzzi[a], L. Bortolotti[b], M. Sbetti[c] and B. Previtali[a]

[a]*Department of Mechanical Engineering, Politecnico di Milano, Via La Masa 1, 20156, Milan, Italy*
[b]*Adige-SYS S.P.A., Viale Venezia 84/b, 38056, Levico Terme (TN), Italy*
[c]*Adige S.P.A., Via per Barco 11, 38056, Levico Terme (TN), Italy*

Abstract

In the industrial practice of the laser cutting, the cut quality is defined in a qualitative manner by skilled technicians. Specific features lying on the cut edges in fact compose the overall quality, i.e. inclination of striations, presence of burr and different process zones along the edge. These attributes are evaluated by experts which at the end assess the cut quality on the base of their personal judgment. On the other hand, measurements of roughness and burr height in accordance to standards or internal procedures are also carried out. However, measuring is time consuming and more important is not always in agreement with the qualitative evaluation given by skilled technicians. In this scenario, the paper presents a method relying on visual information able to measure quantitatively a new class of quality attributes, which opportunely combined provide an index of performance consistent to the qualitative one based on experience.
In this study, images of the cut edge of 5mm thick stainless steel AISI 304 cut with nitrogen as assisting gas are analyzed. The image analysis algorithm utilizes both standard gradient techniques, wavelets decomposition and analyses in the frequency domain for measuring periodic and not periodic quantities. Burr profile is isolated, the typical process zones are successfully identified and striation's angle is computed for each zone. The gray analysis method combining multiple outputs from the image analysis algorithm is applied in order to compute the overall quality. The weights are set to express correctly the judgement of technicians. The method proved reliable, relatively fast and promising for further extension to different thicknesses and materials.

Keywords: laser cutting; quality inspection; gray analysis; image analysis

* Corresponding author. Tel.: +39-02-23998534;
E-mail address: matteo.pacher@polimi.it.

1. Introduction

For many applications and in particular for cutting thin sheet metals, laser cutting has become the reference technology thanks to its flexibility and the gain of productivity if compared with other competitive technologies. However, the proper definition of the process parameters is fundamental for achieving the desired performance (Thomas, 2013). In fact, because of the multi-physics nature of the process for which fluid mechanics is coupled with thermal phenomena, there is a lack of useful models able to reliably predict cut quality; consequently, process parameters have to be adjusted through experimentation.

Assessing quality for the laser cutting process is not trivial: fusion cutting and oxidation cutting produce different features to be evaluated and often there is a lack of classification rules. The reference standard for quality classification, i.e. ISO 9013:2017, classifies cut quality based on roughness (*Rz5*), inclination of the cut edges (*u*) and geometrical tolerances. Among them, the first two parameters describe the quality of the cut edge, whereas the last one the precision of the cutting system and at the end of the produced pieces. In laser fusion cutting it is widely acknowledged that the quantification of the burr height is significant while the inclination of the cut edge plays only a marginal role; in addition, roughness may only be useful to inspect quality among burr-free specimens. Furthermore, some geometrical parameters of the cut edge, e.g. mean angle of the striations and location of the process zones, are usually considered by technicians at least as an aesthetic index of merit.

The quality class defined by the ISO 9013:2017 rarely permits to distinguish cut quality with the same accuracy as the technician's judgement and hence, this classification is not well related with human perceived quality. Accordingly, Librera et al., 2015, showed that visually appreciated differences in the cut edge quality are better represented by an areal measurement of the roughness compared to the standard *Rz5* parameter. Unfortunately, these kinds of measurements are far from being inserted in the usual industrial practice mainly because of long measurement times and high costs of instrumentation. Considering these points, visual sensors have considerable advantages: limited cost, short time required for the whole measuring process and the possibility to develop ad-hoc image analysis algorithms to detect different features.

Thanks to their performance, cameras are more and more adopted in the manufacturing industry. Focusing the attention on quality assessment, Demircioglu et al., 2013, Al-Kindi et al., 2009 and Lee et al., 2005 describe the potentialities of visual algorithms for measuring surface roughness. Unfortunately, these algorithms are based on complex tools such as neural networks which are not easily controllable and strongly depend on the training phase.

The presented study develops a measurement method which is fast and quantitative. The main advantage of the method is that it considers many quality parameters that, opportunely combined, gives a synthetic score which is close to the technicians' judgement.

To avoid unnecessary complexness, an image analysis algorithm was developed based on standard tools to extract multiple outputs and representing the man-observed features. Taking advantage from the studies of Tsai et al., 2009 and Çaydaş et al., 2008, the gray relational analysis was used for combining those outputs. In fact, the gray relational analysis proves effective in the case of a limited number of specimens (Tsai et al., 2009) and it gives a synthetic score which can be easily manipulated.

Finally, the method yields a *relative* measure of quality by construction.

The paper is organized as follows. In Section 2 the information about the experimental setup and procedure are reported. Section 3 describes the measurement algorithm while section 4 reports the main results of the study.

2. Experimental setup

2.1. Experimental equipment

The specimens, AISI 304 stainless steel and 5mm thick, were cut with a BLMGroup LC5 machine equipped with an IPG YLS-6000 laser source with a maximum available power of 6kW and a fiber diameter of 100µm. The cutting head is a Precitec Procutter that has a collimation lens of 100mm and a focal lens of 200mm. Therefore, the laser spot in the waist is equal to 200µm.

Roughness was measured with a linear profilometer (Perthometer Concept MAHR PGK–MAHR PCMESS7024357). To avoid damages, the system was equipped with a 5µm diameter tip and an arm with a 50µm range. The cut-off wavelength for the roughness profile was set to 0.8mm according to the standard ISO 4287:1997.

Images were acquired by a 3D CNC Mitutoyo Vision Measuring System of series Quick Vision ELF. The instrument offers great resolution (0.1µm) and flexibility in setting appropriate light conditions.

2.2. Experimental procedure

A batch of 24 specimens was considered. The specimens were obtained by changing the cutting speed, laser power, focal position as well as gas pressure in order to obtain the largest possible variability of outputs. In other words, all the feasibility window of the process for the mentioned specimens (AISI 304 stainless steel and 5mm) was explored and undesired effects were collected (e.g. burr, high striations' angle, etc.) to properly test the measurement tool. Table 2 summarizes the 24 process parameter conditions.

For each specimen, the Rz5 roughness was measured at three locations, namely *1/3*, *1/2* and *2/3* of the sample thickness, *t*. Each measurement was replicated 3 times in different regions of the specimen. Then Rz5 roughness data were averaged for each location and the maximum *Rz5* value among the three locations was chosen as indicated by the standard ISO 9013:2017. The perpendicularity or angularity tolerance, *u*, reported in the same standard was considered negligible compared to other quality parameters such as burr length and roughness.

A team of four trained operators was asked to evaluate cutting quality in a scale between 0 and 5 and results were averaged to get to a final subjective judgement scale. They basically considered the burr behavior, brightness of the cut edge, regularity of the striation pattern and other qualitative and personal indexes such as the feeling when touching the surface. The quality scale was then normalized between 0 and 1.

Visual information was collected from three images for each specimen in three different locations. The camera in the Mitutoyo Quick Vision ELF was calibrated and hence, the transformation matrix between pixel units and SI units is known. During the image acquisition, the magnification level of the instrument was set to 2.5X.

Finally, light conditions play a crucial role for the reliability of the image analysis algorithm. This is due to some thresholds which must be set for extracting information. To overcome this issue, light conditions were finely tuned in a preliminary stage of the data acquisition process to ensure reliability and consistency of results.

3. Proposed method

As depicted in Fig. 1, the proposed method is in two fundamental steps: the image analysis algorithm and the gray relational analysis.

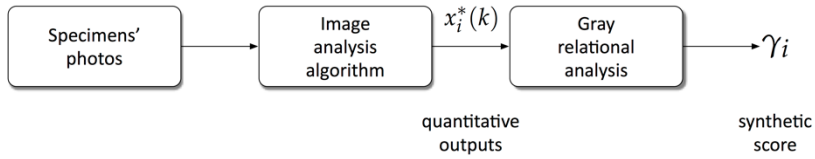

Fig. 1. Scheme of the presented method.

The image analysis algorithm is responsible for extracting data from specimen figures, whereas the gray analysis method is used as described by Çaydaş et al., 2008 among others, to fuse different quantities in a synthetic score.

3.1. Image analysis algorithm

The image analysis algorithm combines different techniques to extract the significant parameters. The aim is to extract the same features analyzed by technicians to combine them later thanks to the gray relational analysis. Since standard techniques for image analysis such as wavelets decomposition, 2D discrete Fourier Transform and gradient based methods are used, the detailed descriptions are not reported for the sake of briefness and we invite the readers to refer to the literature section.

The algorithm is summarized in Fig 2. In the pre-processing phase, input images are adapted to compensate for misalignments in the x-y plane applying proper rotations. Then, burr height, h, is computed thanks to a standard gradient based method. The well-known methods developed by Canny, 1986 for edge detection and Otsu, 1979 for image thresholding were combined to detect the piece outlines in the vertical direction. As a result, the bottom boundary of the piece is computed and the burr height profile is calculated using the information of the calibration matrix. In the second part of the algorithm, the wavelet decomposition is applied to the images and the three process zones are detected by looking at the horizontal details of the image.

As reported by DeBrunner et al., 1999 wavelet transform is an advantageous technique for texture analysis. In fact, the wavelet transform applied to images gives as output directional and frequency information preserving the spatial domain (Olkkonen, 2011).

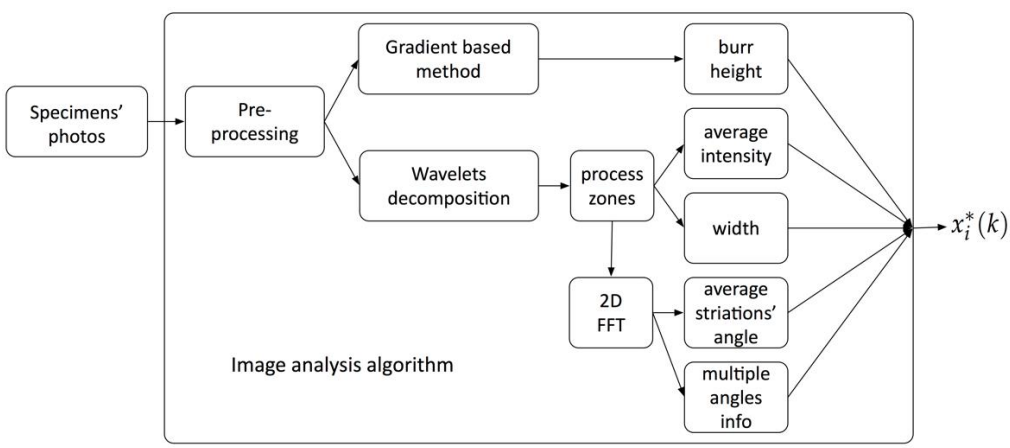

Fig. 2. Block diagram reporting the main steps of the image analysis algorithm.

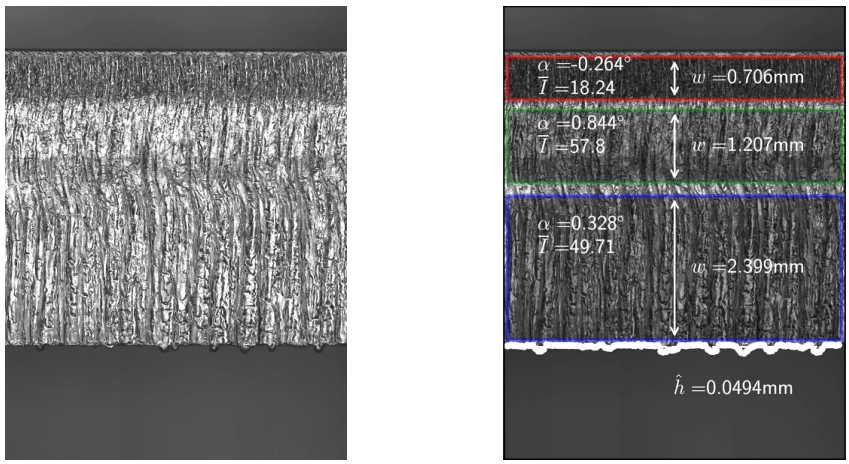

Fig. 3. (a) Original figure of one of the analyzed specimens; (b) Results of the image analysis algorithm for the same image (w represents the zone's width, $\hat{h}$ is the estimate of mean burr height, α is the mean striation's angle and $\bar{I}$ is the average intensity.).

In other words, while the Fourier Transform loses the spatial information about the location of the harmonics, the wavelet transform preserves such information. Once the zones are calculated, width of the three zones (w_1, w_2 and w_3) and average intensity, $\bar{I}$, can be inferred.

The average striation's angle, α, is computed through the fast Fourier transform (FFT) applied to images by analyzing the position of the peaks in the magnitude spectrum. Parallel stripes (e.g. striations) produces a concentration of peaks around their perpendicular direction in the frequency domain. The average angle is computed averaging the angles of each zone. Finally, an additional control variable related to the quality of the fit, η, is extracted; it detects whether striations are well approximated by a line or if their direction is changing along the zone. The extracted quantities are summarized in Table 1.

Table 1. Quantities extracted by the image analysis algorithm and then used in the gray relational analysis.

Nomenclature		
Average burr height	h	[-]
Process zones	$j \in [1,3]$	[-]
Zones' width	w_{j}	[-]
Average intensity	$\bar{I}$	[-]
Striations' average angle	$\alpha = \frac{1}{3}\sum w_j \alpha_j$	[°]
Striations' Fitting control	η	[-]

3.2. Gray relational analysis

In gray relational analysis, multiple outputs are condensed in one single "color" representing the level of information; this technique is used to express the correlation between a desired sequence of outputs and the actual one. This technique is composed by two steps: data pre-processing and gray relational grade calculation.

3.2.1. Data pre-processing

Data pre-processing is a necessary step for transferring original sequences of data into a comparable sequence. In other words, according to the desired performance, each sequence of data is normalized

between zero and one. Given the sequence of data $x_i(k)$ from each of the quantities defined in Table 1, where k represents the quantity and $i \in [1, N]$ the index of the specimens for each sequence, different normalizations are used according to the target value of each sequence. If the target value of the original sequence is as large as possible, the sequence has the characteristic "the-larger-the-better" and is normalized as:

$$x_i^*(k) = \frac{x_i(k) - \min(x_i(k))}{\max(x_i(k)) - \min(x_i(k))}, \quad (1)$$

if the characteristic of the sequence is the-smaller-the-better, the original sequence is normalized as:

$$x_i^*(k) = \frac{\max(x_i(k)) - x_i(k)}{\max(x_i(k)) - \min(x_i(k))}, \quad (2)$$

and finally, if we are interested in a specific target value, x_i^0, the normalization of the original sequence follows as:

$$x_i^*(k) = \frac{|\, x_i(k) - x_i^0 \,|}{\max(x_i(k)) - x_i^0}. \quad (3)$$

According to equations *(1-3)*, in the final normalized data sequences 1 corresponds to the best performance whereas 0 represents the worst one.

3.2.2. Calculation of the gray relational grade

As aforementioned, the gray relational grade expresses the correlation between actual data and reference ones. For this purpose, given $x_0^*(k)$ as the reference sequence indicating the ideal performance for each quantity, the gray relational coefficient is expressed as:

$$\xi_i(k) = \frac{\Delta_{\min} + \zeta \cdot \Delta_{\max}}{\Delta_{0i}(k) + \zeta \cdot \Delta_{\max}}, \quad (4)$$

where $\zeta \in [0, 1]$ is the distinguishing or identification coefficient (usually chosen as $\zeta = 0.5$) and $\Delta_{0i}(k)$ is the deviation sequence, namely:

$$\begin{aligned} \Delta_{0i}(k) &= |x_0^*(k) - x_i^*(k)|, \\ \Delta_{\max} &= \max_{\forall j \in i} \max_{\forall k} |\, x_0^*(k) - x_i^*(k)|, \\ \Delta_{\min} &= \min_{\forall j \in i} \min_{\forall k} |\, x_0^*(k) - x_i^*(k)|. \end{aligned} \quad (5)$$

After obtaining the gray relational coefficient, the gray relational grade is computed via a weighted sum of the coefficients as:

$$\gamma_i = \sum_{k=1}^{N} w_k \cdot \xi_i(k), \qquad \sum_k w_k = 1,\ w_i \in [0, 1]\ \forall\ i = 1, .., k\,. \quad (6)$$

As a result, the gray relational grade is used to evaluate the relationship among the original sequences. The higher the gray relational grade, the closer the comparability sequence is to the reference one. It is here emphasized that the gray relational grade is only a relative measure of how well a comparability sequence fits with the reference one, and no absolute information about quality are available.

3.2.3. Choice of weighting coefficients

The choice of the weighting coefficients, $\boldsymbol{w}$, in equation *(6)* and of the distinguishing coefficient, ζ, in equation (4), represents a non-trivial question. Moreover, in many studies $\boldsymbol{w}$ and ζ are assumed a priori or are set according to author's experience (Ganguly et al., 2012; Lin et al,. 2011).

Since the main goal of this study is to determine a quality measure consistent with the one of technicians, the weighting coefficients were the best-fits weights among the ranking from the gray relational grade and the ranking from the judgement of technicians. This approach was successively validated.

4. Analysis of results

Table 2 reports process parameters, quality and roughness data of the 24 analyzed specimens. Images of the 24 specimens are shown in Table A1. Since *Rz5* = 13µm is the threshold indicated by the ISO 9013:2017 between first and second quality class, all the analyzed data lies in the second quality class (except for sample 10 with a *Rz5* = 12.99µm very close to the threshold). Moreover, a clear correlation between the roughness parameter *Rz5* and the quality expressed by technicians is not found, as Figure 4 shows.

Table 2. Process parameters, measured *Rz5* and personal quality from technicians of the 24 specimens. Columns denoted by "Op. #" report the score given by the four trained operators; quality is computed averaging the four judgements and normalizing to one.

N [-]	Power [W]	Speed [mm/min]	Pressure [bar]	Focal pos. [mm]	Op. 1 [-]	Op. 2 [-]	Op.3 [-]	Op.4 [-]	Quality [-]	*Rz5* (ISO 9013) [µm]
1	6080	6500	16	-1.8	0	0	1	0	0.05	22.24
2	6080	7000	20	-2.5	1	1	2	1	0.25	17.89
3	5800	5500	20	-2.8	1	2	3	1	0.35	21.65
4	2900	2500	19	-4.0	5	4	4	5	0.90	28.83
5	5000	4500	19	-4.0	5	5	4	5	0.95	20.98
6	5000	5500	19	-4.0	3	3	3	4	0.65	16.14
7	6000	6300	19	-4.0	3	2	4	3	0.60	15.05
8	6080	5800	20	-5.0	1	1	2	2	0.30	15.37
9	6080	6000	16	-1.8	0	0	0	0	0.00	21.66
10	6080	5500	16	-6.3	3	3	3	3	0.60	12.99
11	6080	6000	20	-5.5	2	2	1	2	0.35	26.30
12	5500	6000	21	-2.8	3	3	2	3	0.55	17.02
13	5800	6000	20	-2.8	3	2	3	4	0.60	21.40
14	3100	2500	19	-4.0	4	5	5	5	0.95	26.51
15	3000	2500	17	-4.0	4	4	3	4	0.75	25.12
16	6000	5800	19	-4.0	2	3	4	3	0.60	18.52
17	5080	4064	19	-4.0	4	5	5	5	0.95	24.58
18	4080	3709	19	-4.0	4	4	5	4	0.85	24.83
19	6080	5530	19	-5.0	5	5	5	5	1.00	14.50
20	6080	5700	19	-5.5	5	5	5	4	0.95	17.24
21	5080	4200	19	-5.5	5	5	5	5	1.00	21.87
22	5080	4400	19	-5.5	5	4	5	5	0.95	20.38
23	6080	5900	19	-5.5	4	5	4	5	0.90	17.99
24	3080	2800	19	-5.5	4	5	4	4	0.85	21.36

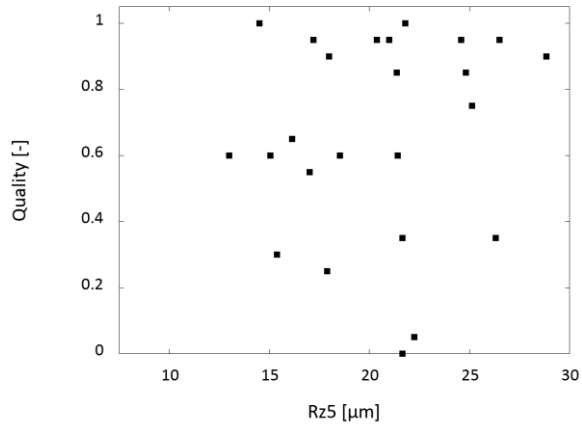

Fig. 4. Normalized quality given by technicians versus the *Rz5* parameter. No clear trends are observed: quality given by technicians considers more parameters other than the roughness.

As a result, the quality classes given by the ISO 9013:2017 standard do not allow to distinguish different levels of laser cut quality while the alone roughness does not represent quality as perceived by technicians.

To set the method, the available 24 specimens were divided in two groups: the first one (16 specimens) was used to calibrate the weights (eq. *(6)*) and the second one (8 specimens) was used to validate the method. Each group contained a set of specimens which was representative of the full scale of quality. The gray relational coefficients ($\xi_i(k)$, eq. *(4)*) were computed from the four quantities (Table 1): average burr height, h, ($k = 1$), average intensity, $\bar{I}$, ($k = 2$), average angle, α, ($k = 3$), and striations' fitting control, η, ($k = 4$). Average angle, fitting control and average burr height have the characteristic the-smaller-the-better, whereas the other two parameters have the characteristic the-larger-the-better.

Fig 5 shows a monotonic trend of quality as a function of the gray relational grade for both the calibration and validation groups: the monotonic trend confirms that the rankings given by the gray relational grade and the technicians' judgement match.

Table 3. Results of the application of the gray analysis on the calibration group. Coefficients of the gray analysis are reported in Table 5.

N [-]	h [mm]	$\bar{I}$ [-]	α [°]	η [-]	$\xi_i(1)$ [-]	$\xi_i(2)$ [-]	$\xi_i(3)$ [-]	$\xi_i(4)$ [-]	γ_i [-]	Quality [-]
19	0.0184	392.48	4.2740	0	0.9594	0.6288	0.5249	1.0	0.8814	1.00
5	0.0134	374.51	5.2703	0	1.0000	0.3833	0.4721	1.0	0.8609	0.95
20	0.0399	394.17	0.7735	0	0.8167	0.6690	0.8652	1.0	0.8541	0.95
17	0.0288	379.26	0.6862	0	0.8846	0.4274	0.8794	1.0	0.8536	0.95
23	0.0639	402.9	1.2837	0	0.7005	1.0000	0.7905	1.0	0.8383	0.90
4	0.0249	340.93	1.2067	0	0.9113	0.2217	0.8010	1.0	0.8294	0.90
24	0.0431	387.57	1.2718	0	0.7991	0.5351	0.7921	1.0	0.8197	0.85
15	0.0450	376.94	0.0458	0	0.7889	0.4047	1.0000	1.0	0.8174	0.75
6	0.0310	383.06	11.7682	0	0.8703	0.4708	0.2850	1.0	0.7934	0.65
16	0.0361	360.69	13.6452	0	0.8388	0.2948	0.2557	1.0	0.7511	0.60
7	0.0580	332.31	14.3781	0	0.7259	0.2000	0.2458	1.0	0.6837	0.60
13	0.0302	361.78	9.8322	1	0.8755	0.3003	0.3231	0.2	0.5438	0.60
11	0.1971	344.71	12.9796	0	0.3913	0.2327	0.2654	1.0	0.5330	0.35
3	0.0422	351.59	13.3893	1	0.8039	0.2559	0.2593	0.2	0.4976	0.35
8	0.3166	349.82	9.6156	1	0.2803	0.2495	0.3280	0.2	0.2575	0.30
1	0.4858	375.11	18.7332	1	0.2000	0.3884	0.2000	0.2	0.2264	0.05

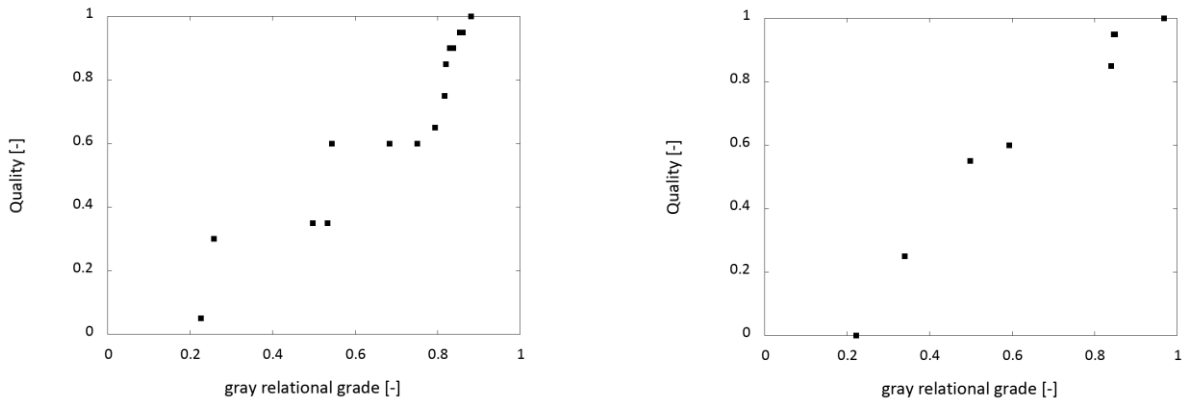

Fig. 5. Normalized quality given by technicians and gray relational grade given combining the outputs of the image analysis algorithm. Results for the calibration (a) and the validation (b) groups.

Data of the calibration and the validation groups are listed in Table 3 and Table 4 respectively; weights are reported in Table 5.

Table 4. Results of the application of the gray analysis on the validation group. Coefficients of the gray analysis are reported in Table 5.

N	$\hat{h}$	$\bar{I}$	$\bar{\alpha}$	η	$\xi_i(1)$	$\xi_i(2)$	$\xi_i(3)$	$\xi_i(4)$	γ_i	Quality
[-]	[mm]	[-]	[°]	[-]	[-]	[-]	[-]	[-]	[-]	[-]
21	0.0188	420.51	2.9484	0	1.0000	1.0000	0.6864	1.0	0.9686	1.00
22	0.0215	366.46	3.0443	0	0.9741	0.2438	0.6773	1.0	0.8497	0.95
14	0.0292	357.17	0.7023	0	0.9072	0.2158	1.0000	1.0	0.8466	0.95
18	0.0342	382.32	0.7735	0	0.8684	0.3134	0.9857	1.0	0.8406	0.85
10	0.1143	352.87	11.0858	0	0.5156	0.2049	0.3213	1.0	0.5931	0.60
12	0.0577	396.78	7.8389	1	0.7232	0.4235	0.4078	0.2	0.4980	0.55
2	0.1212	350.79	20.3638	1	0.4982	0.2000	0.2000	0.2	0.3401	0.25
9	0.4254	360.06	8.5602	1	0.2000	0.2238	0.3848	0.2	0.2218	0.00

Table 5. Coefficients used in the gray analysis (eq. *(4)* and eq. *(6)*).

ζ	w_1	w_2	w_3	w_4
[-]	[-]	[-]	[-]	[-]
0.25	0.47	0.14	0.10	0.29

5. Conclusions

The presented method proved effective for ranking 5mm thick AISI 304 specimens according to their relative quality. The method overcomes the issue of subjective quality assessment given by technicians and may help technicians to rank between specimens having quality really close to each other. In addition, since

many parameters are considered, the method gives a quality ranking closer to the one of technicians if compared with standard ISO 9013:2017.

Future developments regard the extension of the presented method to different thicknesses and other materials cut with nitrogen as assisting gas. Different metallic alloys in fact, namely carbon steels as well as aluminum and copper based alloys, manifest similar features once laser cut with nitrogen. Conversely, thickness plays an important role in the feature generation. In particular, the method should be tested for very thin thicknesses (from 0 to 3-4mm) where features are either not present or cannot be easily distinguished.

While the method can give only a relative measure of quality i.e. the ranking of the analyzed specimens, absolute quality assessment remains a research question. Future developments will focus on this point and on the possibility of integrating machine learning algorithms for the automatic optimization of process parameters.

Acknowledgements

The project presented in this paper has been funded with the contribution of the Autonomous Province of Trento, Italy, through the Regional Law 6/98. Name of the granted Project: LT4.0.

References

Al-Kindi, Ghassan A., and Bijan Shirinzadeh, 'Feasibility Assessment of Vision-Based Surface Roughness Parameters Acquisition for Different Types of Machined Specimens', *Image and Vision Computing*, 27 (2009), 444–58 Canny, John, 'A Computational Approach to Edge Detection', *IEEE Transactions on Pattern Analysis and Machine Intelligence*, PAMI-8 (1986), 679–98

Çaydaş, Ulaş, and Ahmet Hasçalik, 'Use of the Grey Relational Analysis to Determine Optimum Laser Cutting Parameters with Multi-Performance Characteristics', *Optics and Laser Technology*, 40 (2008), 987–94

DeBrunner, V., and M. Kadiyala, 'Texture Classification Using Wavelet Transform', in *42nd Midwest Symposium on Circuits and Systems (Cat. No.99CH36356)* (IEEE, 1999), II, 1053–56

Demircioglu, Pinar, Ismail Bogrekci, and Numan M. Durakbasa, 'Micro Scale Surface Texture Characterization of Technical Structures by Computer Vision', *Measurement: Journal of the International Measurement Confederation*, 46 (2013), 2022–28

Ganguly, D., B. Acherjee, A. S. Kuar, and S. Mitra, 'Hole Characteristics Optimization in Nd:YAG Laser Micro-Drilling of Zirconium Oxide by Grey Relation Analysis', *International Journal of Advanced Manufacturing Technology*, 61 (2012), 1255–62

Lee, Kuang-chyi, Shinn-jang Ho, and Shinn-ying Ho, 'Accurate Estimation of Surface Roughness from Texture Features of the Surface Image Using an Adaptive Neuro-Fuzzy Inference System', *Precision Engineering*, 29 (2005), 95–100

Librera, Erica, Giovanni Riva, Hossein Safarzadeh, and Barbara Previtali, 'On the Use of Areal Roughness Parameters to Assess Surface Quality in Laser Cutting of Stainless Steel with CO2 and Fiber Sources', *Procedia CIRP*, 33 (2015), 532–37

Lin, Shun Te, Shi Jinn Horng, Bih Hwang Lee, Pingzhi Fan, Yi Pan, Jui Lin Lai, and others, 'Application of Grey-Relational Analysis to Find the Most Suitable Watermarking Scheme', *International Journal of Innovative Computing, Information and Control*, 7 (2011), 5389–5401

Olkkonen, Juuso, *Discrete Wavelet Transforms - Theory And Applications*, *Book* (Intech, 2011)

OTSU, N., 'A TIreshold Selection Method from Gray-Level Histograms', *Transaction on Systems, Man, and Cybernetics*, 20 (1979), 62–66

Thomas, Daniel J., 'The Effect of Laser Cutting Parameters on the Formability of Complex Phase Steel', *The International Journal of Advanced Manufacturing Technology*, 64 (2013), 1297–1311

Tsai, Ming Jong, and Chen Hao Li, 'The Use of Grey Relational Analysis to Determine Laser Cutting Parameters for QFN Packages with Multiple Performance Characteristics', *Optics and Laser Technology*, 41 (2009), 914–21

Appendix A. Images of the specimens

Table A1. Images of the 16 specimens used for calibrating the method. Process parameters are reported in Table 1.